Published in final edited form as:
Traffic. 2010 August ; 11(8): 1056–1066. doi:10.1111/j.1600-0854.2010.01074.x.

MAL2 Selectively Regulates Polymeric IgA Receptor Delivery from the Golgi to the Plasma Membrane in WIF-B cells

Julie G. In and **Pamela L. Tuma***
Department of Biology, The Catholic University of America, Washington, DC 20064

Abstract

MAL2 has been identified as a hepatic transcytotic regulator that mediates delivery from basolateral endosomes to the sub-apical compartment (SAC). However, overexpression of polymeric immunoglobulin A-receptor (pIgA-R) in polarized, hepatic WIF-B cells led to the dramatic redistribution of MAL2 into the Golgi and all the transcytotic intermediates occupied by the receptor. Although overexpressed hemagglutinin and dipeptidylpeptidase IV (DPPIV) distributed to the same compartments, MAL2 distributions did not change indicating the effect is selective. Cycloheximide treatment led to decreased pIgA-R and MAL2 intracellular staining, first in the Golgi then the SAC, suggesting they were apically delivered and that MAL2 was mediating the process. This was tested in Clone 9 cells (that lack endogenous MAL2). When expressed alone, pIgA-R was restricted to the Golgi whereas when coexpressed with MAL2, it distributed to the surface, was internalized and delivered to MAL2-positive puncta. In contrast, DPPIV distributions were independent of MAL2. Surface delivery of newly synthesized pIgA-R, but not DPPIV, was enhanced >9-fold by MAL2 coexpression. In WIF-B cells where MAL2 expression was knocked down, pIgA-R, but not DPPIV, was retained in the Golgi and its basolateral delivery was impaired. Thus, in addition to its role in transcytosis, MAL2 also regulates pIgA-R delivery from the Golgi to the plasma membrane.

Keywords

apical sorting; MAL2; pIgA-R; WIF-B cells; hepatocytes

The plasma membrane of polarized hepatic cells is physically continuous but functionally and compositionally divided into two domains: the apical and basolateral (reviewed in 1). These domains are characterized by distinct and specialized functions. For example, functions at the apical domain include the apical excretion of bile acids, biliary lipids, detoxification products, and the delivery of immunoglobulin A (IgA) whereas functions at the basolateral domain include the transport of amino acids and glucose, secretion of plasma and lipoproteins and internalization of circulating macromolecules from the blood (1). These domain-specific activities require the presence of distinct plasma membrane proteins; few proteins distribute equally between both domains. How is this polarity established and maintained? The answer comes, in part, from understanding polarized membrane trafficking. Our focus is to understand the mechanisms regulating apical delivery of newly synthesized apical proteins in polarized hepatocytes.

Unlike most simple epithelial cells, hepatocytes use an indirect pathway for apical delivery of newly synthesized single transmembrane domain and glycophosphatidylinositol (GPI) anchored proteins (2–4). They are first delivered from the TGN to the basolateral domain

*Corresponding author: ph: 202-319-6681, FAX: 202-319-5721, tuma@cua.edu.

where they are selectively retrieved by endocytosis and transcytosed to the apical membrane (2–4). Previously, we determined that transcytotic efflux from early endosomes to the sub-apical compartment (SAC) in polarized, hepatic WIF-B cells required cholesterol and glycosphingolipids (5). Depletion of these lipids impaired the efflux of *all* apical residents examined and polymeric IgA-receptor (pIgA-R), irrespective of their detergent solubility properties (5). Thus, we proposed that the lipid-dependent early endosome sorting was conferred by a general regulator of transcytosis whose activity requires both cholesterol and glycosphingolipids.

We have initiated studies to examine whether the *m*yelin *a*nd *l*ymphocyte protein 2 (MAL2) is a good candidate for mediating this lipid-dependent transport step. This 19 kDa tetraspanning membrane protein is lipid-associated and has been implicated in regulating transcytosis (6). In HepG2 cells, antisense MAL2 oligonucleotides impaired transcytosis of two classes of apical proteins: pIgA via its single spanning receptor and CD59, a GPI-anchored protein (6). Interestingly, the block occurred between the early endosome and SAC, reminiscent of the block we observed in lipid-depleted WIF-B cells. Thus, we propose that lipid depletion prevented MAL2 from sorting transcytosing proteins at early endosomes.

To begin our studies on MAL2, we generated specific antibodies, and determined that MAL2 was mainly localized to the apical membrane and SAC in WIF-B cells mostly consistent with reports from others (6–10). We further discovered that overexpression of pIgA-R, but not the single spanning apical residents, dipeptidyl peptidase IV (DPPIV) or hemagglutinin (HA), led to the remarkable redistribution of MAL2 from the apical membrane into the biosynthetic and transcytotic intermediates also occupied by the receptor. From the studies reported here, we conclude that in addition to its proposed role in the regulation of transcytosis from early endosomes to the SAC, MAL2 also selectively regulates pIgA-R delivery from the Golgi to the basolateral plasma membrane.

Results

MAL2 is an itinerant protein in WIF-B cells

To begin our studies, we generated anti-MAL2 polyclonal peptide antibodies against a divergent and specific 11 amino acid N-terminal span in rat MAL2 (11). On immunoblots in WIF-B cells, our antibodies detected a 19 kDa species (the predicted MAL2 molecular weight), a band at 25 kDa (marked by an asterisk) and a diffuse set of bands ranging from 30–38 kDa (Figure 1A). The 25 kDa band and the diffuse bands have been detected by others using different custom antibodies and have been postulated to be glycosylated forms of MAL2 (6, 10). To further confirm specificity of our antibody, we blotted lysates from control or MAL2-overexpressing Clone 9 cells. Importantly, these hepatic-derived, nonpolarized cells lack endogenous MAL2 expression. As shown in Figure 1A, MAL2 was detected only in Clone 9 cells that were overexpressing MAL2 confirming antibody specificity. As for WIF-B cells, a 19 kDa band, a 25 kDa band and the higher molecular weight cluster were detected, although the latter two species were less abundant suggesting differential protein processing in the two cell types.

In WIF-B cells, the MAL2 antibodies labeled structures at or near the bile canaliculi (BC), and this labeling was lost after preabsorption with the N-terminal MAL2 peptide used to generate the antibodies (Figure 1B). Importantly, canalicular staining of the GPI-anchored apical resident, 5'nucleotidase (5'NT), was not changed when preabsorbed with the peptide further indicating our reagent is specific (Figure 1B). Moreover, labeling was detected only in Clone 9 cells infected with recombinant MAL2 adenovirus. Staining at both the plasma membrane and in intracellular puncta was observed (Figure 1C and see Figure 5).

Although MAL2 labeling at the apical pole has been reported by others (6–10), this location is not necessarily predicted based on MAL2's proposed role in transcytotic sorting from the basolateral early endosome to the SAC. One explanation is that MAL2 is an itinerant protein cycling among the transcytotic intermediates, a possibility that has been confirmed by live cell imaging in HepG2 cells overexpressing GFP-tagged MAL2 (7). To confirm that *endogenous, untagged* MAL2 is itinerant in WIF-B cells, we chose a pharmacological approach to stage MAL2 in various transcytotic intermediates. First, we treated WIF-B cells for 1 h with 5 mM methyl-β–cyclodextrin (mβCD), conditions that deplete 80% of cholesterol in WIF-B cells and block transcytotic efflux of apical proteins from early endosomes (5). As for the apical residents in cholesterol-depleted cells (5), MAL2 staining was no longer restricted to the apical pole; basolateral labeling was also observed (Figure S1b).

We next used two manipulations that have been shown to alter SAC function and/or morphology. The first was an 18°C temperature block that has been reported to impair transport from the SAC (12), and the second was adding nocodazole that is reported to vesiculate the SAC (13). As shown in Figure S1c, after the temperature block, MAL2 staining was found primarily in structures just adjacent to the apical membrane with a reciprocal decrease in apical labeling suggesting it redistributed to the SAC. In nocodazole-treated cells, MAL2 was observed in vesiculated structures emanating from the apical surface with decreased labeling at the BC (Figure S1d) also suggesting MAL2 is present in the SAC.

To further confirm that MAL2 traverses the SAC, we determined the distribution of trafficked endolyn relative to that of MAL2 at steady state. Basolaterally internalized endolyn is delivered to the SAC before its transport to lysosomes providing a useful marker for this transcytotic intermediate (14). The basolateral pool of endolyn was continuously labeled with antibodies for 1 h and then visualized with secondary antibodies. As shown in Figure S1f, a substantial proportion of the endolyn population was present near the apical surface in the SAC (14). MAL2 steady state labeling significantly overlapped with the sub-apically located endolyn indicating that a subpopulation of MAL2 resides in the SAC. Similarly, MAL2 colocalized with basolaterally labeled 5'NT present in the SAC after 1 h of uptake (Figure S1 g and h). Together these results indicate that like overexpressed, GFP-tagged MAL2 in HepG2 cells (7), endogenous, untagged MAL2 in WIF-B cells is itinerant and can be staged in various transcytotic compartments (basolateral membrane, SAC and apical membrane).

MAL2 and overexpressed pIgA-R selectively colocalize and coimmunoprecipitate

We next examined MAL2 distributions in WIF-B cells overexpressing pIgA-R and other single spanning apical residents. Surprisingly, overexpression of pIgA-R led to the remarkable redistribution of MAL2 into nearly all of the compartments occupied by the receptor (Figure 2A, a–c). Only the diffuse ER-like pIgA-R staining pattern was not observed for MAL2. When cells were treated with nocodazole and focused above the nuclear plane, near perfect colocalization was seen in peripherally located structures (Figure 2A, d–f). Interestingly, overexpression of the single spanning apical ectoenzyme, DPPIV, did not lead to MAL2 redistribution despite its presence in the same compartments as pIgA-R (albeit with higher levels of diffuse ER-like staining) (Figure 2A, g–i). Although DPPIV was found in punctuate structures in nocodazole-treated cells when images were focused at the nuclear plane, no DPPIV was present in the MAL2 positive peripheral structures as seen with pIgA-R (Figure 2A, j–l). When quantitated, we determined that almost 88% of polarized cells positive for intracellular populations of pIgA-R were also positive for MAL2 intracellular labeling whereas only ~12% of polarized cells positive for intracellular DPPIV were also positive for intracellular MAL2 (Figure 2B). Similarly, HA overexpression did not

alter MAL2 distributions (data not shown) suggesting selective interactions between MAL2 and pIgA-R.

The near perfect colocalization of pIgA-R and MAL2 at steady state suggested the proteins were directly interacting. To test this possibility, we performed coimmunoprecipitations in cells overexpressing pIgA-R. We first tested our antibodies for specific MAL2 immunoprecipitation. As shown in Figure S2A, the affinity purified antibodies specifically immunoprecipitated a 19 kDa protein from WIF-B whole cell extracts (WCE). There was no immunoreactive species in samples incubated without addition of cell extract, and addition of the N-terminal peptide used to generate the antibodies blocked MAL2 immunoprecipitation. We also determined that 1 μg of affinity purified MAL2 antibodies quantitatively recovered MAL2 from lysates; no additional binding was observed with 5 μg (Figure S2B).

As shown in Figure 2C, exogenous pIgA-R coimmunoprecipitated with anti-MAL2. Importantly, no pIgA-R was detected in immunopreciptations using preimmune MAL2 sera even on overexposed immunoblots (Figure S2C). Interestingly, only the higher molecular weight, mature form of the receptor was detected in the MAL2 bound fractions (Figure 2C), even after prolonged exposure (Figure S2D), consistent with the lack of MAL2 colocalization with pIgA-R in the diffuse, ER-like structures (Figure 2A, a–c). This result further indicates that MAL2-pIgA-R interactions are occurring in a late- or post-Golgi compartment. Consistent with the lack of MAL2 redistribution in DPPIV overexpressing cells, no exogenous DPPIV was recovered in MAL2 immunoprecipitates (Figure 2C).

A population of the intracellular structures occupied by pIgA-R and MAL2 appeared Golgi-like. To confirm this, we double labeled pIgA-R overexpressing cells with albumin, a hepatic Golgi marker. As shown in Figure 3A, there was significant overlap of staining in the intracellular structures confirming their Golgi identity. To further confirm that MAL2 and pIgA-R were present in biosynthetic organelles, we treated cells with cycloheximide. In cells treated for 30 min, the Golgi staining of both MAL2 and pIgA-R was diminished and sub-apical structures were observed (Figure 3B, d–f), and by 60 min, only apical labeling was detected (Figure 3B, g–i). This “chase” from the intracellular structures to the apical membrane suggests that MAL2 and pIgA-R were interacting along the transcytotic route including transport from the Golgi to the basolateral membrane.

We quantitated cells positive for intracellular staining of MAL2 and pIgA-R to confirm these observations. At 0 min, 100% of infected polarized cells contained intracellular pIgA-R populations and ~80% of these cells were also positive for intracellular MAL2. After 30 min, ~50% cells contained intracellular MAL2 and pIgA-R, and by 60 min, only ~35% cells had intracellular MAL2 populations (Figure 3C). Because cells were scored “negative” or “positive” only, the high pIgA-R expression levels prevented complete loss of intracellular labeling after 60 min. Nonetheless, we conclude that pIgA-R and MAL2 traverse the transcytotic pathway together starting at the Golgi. To determine whether pIgA-R overexpression induced MAL2 biosynthesis, and thus its appearance in the Golgi, we immunoblotted control and overexpressing cell lysates for MAL2 levels. No changes in MAL2 protein levels were detected indicating that the MAL2 Golgi reflects a redistribution, not an induction, in pIgA-R overexpressing cells (Figure 3D).

MAL2 regulates delivery from the Golgi to the plasma membrane

The unexpected redistribution of MAL2 into the Golgi in pIgA-R overexpressing cells and the “chase” of both the receptor and MAL2 from the Golgi in cycloheximide-treated cells within 60 min suggested that MAL2 was regulating pIgA-R delivery from the TGN to the basolateral membrane. To test this possibility, we first examined pIgA-R and DPPIV

dynamics in nonpolarized WIF-B cells and nonpolarized, hepatic Clone 9 cells. Importantly, the nonpolarized WIF-B cells express endogenous MAL2 and apical proteins whereas Clone 9 cells do not.

In nonpolarized WIF-B cells, apical proteins distribute to an intracellular compartment that contains only other apical residents (5, 16). We have rigorously characterized this compartment and determined that it contains only other apical proteins. So far, GPI-anchored apical residents, single spanning ectoenzymes, the polytopic transporter, MRP2, and pIgA-R have been shown to reside in this apical compartment (5, 16). In contrast, markers for recycling endosomes, early endosomes, lysosomes, late endosomes, Golgi and the basolateral surface are excluded from this compartment (5, 16). As predicted by its apical location in WIF-B cells, MAL2 was also present in this so-called "apical compartment" in nonpolarized WIF-B cells (Figure S3). Our previous studies have also shown that apical proteins in nonpolarized hepatic cells rapidly recycle between the apical compartment and the cell surface (5, 16). By monitoring the trafficking of antibody-labeled DPPIV and pIgA-R to the intracellular structures, we further determined that MAL2 localized to the same compartment to which the apical proteins are delivered (Figure S3).

We next examined the distributions of exogenously expressed DPPIV and pIgA-R in Clone 9 cells that lack endogenous expression of apical proteins and MAL2. Previously, we determined that overexpressed DPPIV distributed to an analogous "apical compartment" in Clone 9 cells (5, 16) in the absence of MAL2. To confirm that this apical compartment also received apical proteins internalized from the cell surface, we antibody labeled DPPIV present at the plasma membrane at 4°C and chased the antibody-antigen complexes for 1 h at 37°C. As shown in Figure 4A (a), internalized DPPIV was detected at intracellular structures. To determine whether DPPIV recycled between this compartment and the plasma membrane, we first staged DPPIV in the compartment. The remaining plasma membrane-associated antibodies were stripped with isoglycine and only the internalized antibody-antigen complexes were protected and thus, detected (Figure 4A, b). After an additional hour at 37°C, DPPIV was detected at the plasma membrane indicating that it recycled to the surface (Figure 4A, c). Staining of nonpermeabilized cells that were processed in parallel (Figure 5, d–f) verified these observations.

Unlike DPPIV, pIgA-R distributed mainly to the Golgi in Clone 9 cells (Figure 4B, a and b). To determine whether a subpopulation of pIgA-R was delivered to the plasma membrane and then delivered to the apical compartment, we continuously labeled Clone 9 cells with anti-pIgA-R antibodies for 1 h. However, no intracellular staining was observed (Figure 4B, c). To confirm that pIgA-R was not present at the plasma membrane in Clone 9 cells, we surface labeled cells with biotin at 4°C. Only DPPIV was recovered with streptavidin agarose; no pIgA-R was detected in the bound fractions (Figure 4C) even after prolonged exposure (data not shown). These results indicate that pIgA-R is retained in the Golgi in the absence of MAL2 in Clone 9 cells.

In contrast, when MAL2 was coexpressed in Clone 9 cells, pIgA-R distributed to the MAL2-positive apical compartment and the plasma membrane (Figure 5A, a–c). Double labeling with mannosidase II further confirmed that the intracellular puncta were not the Golgi (Figure 5A, d–f). To confirm that pIgA-R was delivered to the plasma membrane in MAL2 expressing cells, we surface labeled cells with biotin as described for Figure 4. Virtually no pIgA-R (~0.6% of total) was detected at the plasma membrane in cells without MAL2 (Figure 5B). In striking contrast, surface delivery of pIgA-R was greatly enhanced (> 9-fold) in MAL2 coexpressing cells (Figure 5B). For comparison, we monitored DPPIV delivery in singly infected cells or in cells coexpressing MAL2. As shown in Figure 5B, no change in plasma membrane association was observed indicating that DPPIV distributions

are MAL2 independent. To determine whether pIgA-R was delivered from the cell surface to the apical compartment, we continuously labeled MAL2 coexpressing cells with anti-pIgA-R for 1 h. As shown in Figure 5C, pIgA-R was robustly internalized and delivered to intracellular structures that were also positive for MAL2 at steady state (Figure 5C, a–c). Thus, in MAL2 coexpressing cells, pIgA-R distributed to the apical compartment and recycled between it and the cell surface.

To monitor Golgi to plasma membrane delivery directly, we measured plasma membrane association of a pIgA-R cohort in cycloheximide-treated Clone 9 cells using surface biotinylation. In cells overexpressing only pIgA-R, there was virtually no receptor detected at the plasma membrane for any time point indicating very low levels of surface expression consistent with our morphological observations (Figure 6A). In contrast, significant plasma membrane labeling was observed in cells expressing MAL2 (Figure 6A) that decreased after prolonged exposure in cycloheximide (Figure 6B). After 90 min of chase, only 68% of pIgA-R remained at the cell surface indicating the newly synthesized pIgA-R had traversed the plasma membrane and was delivered to the intracellular “apical” structures. In comparison, DPPIV surface association did not change in cells expressing MAL2 (Figure 6B). In both cases, decreased DPPIV was detected in the plasma membrane in cycloheximide-treated cells (Figure 6B and data not shown). Thus, we conclude that MAL2 selectively regulates delivery of pIgA-R from the Golgi to the plasma membrane.

We confirmed these results in polarized WIF-B cells where MAL2 expression was knocked down. Because WIF-B cells are recalcitrant to transfection with conventional reagents to introduce oligonucleotides or siRNA, we chose an anti-sense approach using recombinant adenovirus. After 20 h of infection, MAL2 levels were decreased to 38% of control (Figure 7A). Although this incomplete knockdown precluded quantitative biochemical analysis, morphological examination of MAL2 knockdown cells was performed. In control cells, pIgA-R was detected in the same biosynthetic and transcytotic structures as described in Figure 2 (Figure 7C, a). However, in cells where MAL2 expression was knocked down, pIgA-R was detected only in the Golgi. Two examples are shown in Figure 7C (b–e). The percent cells exhibiting basolateral populations of pIgA-R was calculated for cells where MAL2 expression was not detected (−), somewhat visible (−/+) or present at normal levels (+) (Figure 7B). In cells with complete MAL2 knockdown, no basolateral receptor populations were observed whereas in cells expressing endogenous MAL2 levels, almost 100% of cells were positive for basolateral pIgA-R staining. In contrast, DPPIV distributions were not changed in MAL2 knockdown cells (Figure 7D). In both control and knockdown cells, intracellular and apical membrane distributions of DPPIV were observed. When quantitated, 100% of cells for all three MAL2 expression levels were positive for basolateral DPPIV labeling (Figure 7B).

We next examined transcytosis of DPPIV and pIgA-R in MAL2 knockdown cells. Cells were antibody labeled at 4°C and the antibody-antigen complexes chased for 1 h at 37°C. Basolateral labeling at 4°C of both DPPIV (Figure 8A, a) and pIgA-R (Figure 8B, a) was observed in control cells, and after 1 h of chase, both proteins were delivered to the apical membrane with a reciprocal decrease in basolateral labeling indicating successful transcytosis (Figures 8A, f and 8B, h). In MAL2 knockdown cells, DPPIV basolateral labeling at 4°C was not changed (two examples are shown in Figure 8A) indicating its TGN to surface delivery is MAL2 independent. Consistent with MAL2’s known role in transcytosis from early endosomes to the SAC (6), the apical delivery of DPPIV was impaired in MAL2 knockdown cells (Figure 8A, g and h) and intracellular puncta were observed (Figure 8A, g, marked with arrows).

In contrast, no pIgA-R labeling was detected in MAL2 knockdown cells (Figure 8B, d) consistent with impaired basolateral delivery. However, some pIgA-R surface labeling was detected in cells where MAL2 expression was only partially knocked down. Two examples are shown in Figure 8B (b and c). The percent cells with basolateral pIgA-R populations was calculated, and in cells with complete MAL2 knockdown, no basolateral receptor populations were observed. However, in cells expressing low or endogenous MAL2 levels, basolateral pIgA-R labeling was observed (Figure 8C). After 1 h of chase, no pIgA-R was detected in cells with complete MAL2 knockdown consistent with a lack of surface labeling at 4°C. However, in cells with partial MAL2 knockdown, pIgA-R apical delivery was impaired and the receptor was detected in intracellular puncta (Figure 8B, i; marked with arrows) confirming that MAL2 regulates pIgA-R transcytosis (6).

Discussion

We began these studies with the intention of studying the role of MAL2 in lipid-dependent transcytotic sorting at the early endosome. However, the observation that endogenous MAL2 redistributed to the Golgi in pIgA-R overexpressing cells and was “chased” to the apical membrane along with the receptor led us to examine whether MAL2 also functions in plasma membrane delivery from the Golgi. Our studies in Clone 9 cells (that lack endogenous MAL2 expression) and in polarized WIF-B cells with MAL2 expression knocked down revealed that MAL2 selectively mediates transport of pIgA-R from the Golgi to the plasma membrane. Thus, MAL2 regulates multiple steps of pIgA-R’s cellular itinerary.

MAL2 and overexpressed pIgA-R selectively colocalize and coimmunoprecipitate

Overexpression of pIgA-R led to the remarkable redistribution of MAL2 into nearly all of the compartments occupied by the receptor, only the diffuse ER-like pIgA-R staining pattern was not observed for MAL2. This near perfect colocalization at steady state and during “chase” with cycloheximide suggests the proteins interact directly, and this was confirmed with coimmunoprecipitations. Only the mature form of pIgA-R coimmunoprecipitated with MAL2; DPPIV was not recovered. We determined that ~1% of total pIgA-R coimmunoprecipitated with MAL2 consistent with results from MDCK cells where only 0.7–2% of MAL coimmunoprecipitated with overexpressed HA (17). These results suggest that MAL2-pIgA-R interactions are likely weak, transient or indirect. Because MAL2 has been shown to bind members of the TPD52 family of proteins (11, 18), and because these proteins have been implicated in Ca^{2+}-dependent regulation of pancreatic apical secretion (19–21), we favor the latter possibility. We are currently identifying MAL2 binding partners to further examine MAL2 interactions with pIgA-R and other apical proteins.

A new role for MAL2?

To test whether MAL2 selectively regulated transport from the TGN to the Golgi, we examined pIgA-R and DPPIV dynamics in nonpolarized WIF-B cells, Clone 9 cells, and in polarized WIF-B cells where MAL2 expression was knocked down. In nonpolarized WIF-B cells, apical proteins recycle between the plasma membrane and an intracellular compartment that contains only other apical residents. We have rigorously characterized this so-called “apical compartment” and determined that it contains only other apical proteins; markers for recycling endosomes, early endosomes, lysosomes, late endosomes, Golgi and basolateral membranes are excluded (5, 16). In this study, we further determined that MAL2 is present in this apical compartment.

In Clone 9 cells, we previously determined that DPPIV is present in an analogous “apical compartment” and displays similar recycling properties (5, 16). Surprisingly, and unlike

DPPIV, pIgA-R distributed only to the Golgi in Clone 9 cells in the absence of MAL2 expression. Similarly, in WIF-B cells where MAL2 expression was knocked down, pIgA-R distributed predominantly to the Golgi. In contrast, when MAL2 was coexpressed in Clone 9 cells, pIgA-R distributed from the Golgi into the MAL2 positive apical compartment after traversing the plasma membrane. Thus, in MAL2 coexpressing cells, pIgA-R was delivered to the apical compartment and recycled between it and the cell surface. When surface delivery was measured in cycloheximide-treated cells, we further determined that MAL2 coexpression was required for pIgA-R delivery from the Golgi to the plasma membrane.

In 2002, de Marco and colleagues established that MAL2 is a regulator of hepatic transcytosis in HepG2 cells (6). By using antisense oligonucleotides, they showed that MAL2 knockdown resulted in a block in transport from early endosomes to SAC of both pIgA and the GPI-anchored protein, CD59. Similarly, transcytosis of DPPIV in WIF-B cells lacking MAL2 expression was impaired. However, our finding that pIgA-R basolateral delivery is impaired in complete MAL2 knockdown WIF-B cells is not consistent with the HepG2 studies. If MAL2 knockdown also impairs pIgA-R basolateral delivery in HepG2 cells, the expectation is that there would be no receptor present to internalize the added ligand. One possible explanation is that the block in Golgi exit was not complete in the MAL2 knockdown HepG2 cells allowing some pIgA-R basolateral delivery. This is consistent with our findings that in cells with partial MAL2 knockdown, some pIgA-R is basolaterally delivered and internalized. Differences in approach i.e., monitoring the receptor directly (in WIF-B cells) vs. the ligand (in HepG2 cells) may also explain these disparate results. Another possibility is that there are cell type differences in MAL2 regulation of pIgA-R trafficking. Clearly, further research is needed to define the role(s) of MAL2 in apical targeting not only in hepatic cells, but also in other polarized epithelial cell types.

Nonetheless, our results together with results from HepG2 cells suggest that MAL2 can regulate at least two steps in the itinerary of pIgA-R: transcytotic delivery from the early endosome to the SAC and delivery from the TGN to the basolateral membrane. Interestingly, a highly related family member, MAL, has been found to regulate the itineraries of apical proteins at two transport steps in MDCK cells: direct delivery from the TGN to the apical membrane and apical internalization (22–24). Thus, MAL family members are likely multifunctional proteins, and we predict the list of transport steps that these proteins regulate in the itineraries of apical proteins will expand as further study continues.

MAL2 regulation of plasma membrane delivery is selective

What is the basis of selectivity for MAL2 in mediating pIgA-R Golgi to basolateral transport? One possibility is the different cytoplasmic sequences on pIgA-R vs. HA and DPPIV promote different interactions with MAL2. The 103 amino acid pIgA-R cytoplasmic domain encodes multiple known targeting signals that mediate its delivery to the basolateral membrane and basolateral internalization, that stimulate transcytosis and prevent lysosomal degradation (25–29 and reviewed in 1). In contrast, DPPIV and HA encode short, cytoplasmic tails (6 or 12 amino acids, respectively) that contain no known targeting information. Interestingly, when MAL was overexpressed in WIF-B cells (that lack endogenous MAL), HA and DPPIV were rerouted to the apical membrane via the direct route whereas indirect pIgA-R sorting was not altered (30). We proposed at the time that the basolateral targeting information in the pIgA-R cytoplasmic domain was dominant thereby preventing interactions with MAL and eluding redirection. An exciting possibility is that the basolateral targeting information is dominant because it mediates interactions (directly or indirectly) with MAL2 at the Golgi, a hypothesis we are currently testing.

Materials and Methods

Reagents and antibodies

Nocodazole, F12 (Coon's modification) medium, mβCD, cycloheximide and streptavidin agarose were purchased from Sigma-Aldrich (St. Louis, MO). NHS biotin was purchased from Pierce (Rockford, IL). Fetal bovine serum (FBS) was purchased from Gemini Bio-Products (West Sacramento, CA). HRP-conjugated secondary antibodies and Western Lightning chemiluminescence reagent were from Sigma-Aldrich and PerkinElmer (Crofton, MD), respectively. Alexa-conjugated secondary antibodies were purchased from Invitrogen (Carlsbad, CA). Antibodies against pIgA-R, DPPIV, endolyn and 5'NT were generously provided by Dr. A. Hubbard (Johns Hopkins University, School of Medicine, Baltimore, MD). Recombinant adenoviruses encoding V5/His6 epitope-tagged full-length pIgA-R, V5/myc epitope-tagged full-length DPPIV and full-length HA were also provided by Dr. A. Hubbard and have been described in detail (31).

Cell culture

WIF-B cells were grown in a humidified 7% CO_2 incubator at 37°C as described (32). Briefly, cells were grown in F12 medium (Coon's modification), pH 7.0, supplemented with 5% FBS, 10 μM hypoxanthine, 40 nM aminoterpin and 1.6 μM thymidine. Clone 9 cells were grown at 37°C in a 5% CO_2 incubator in F12 medium supplemented with 10% FBS. WIF-B cells were seeded onto glass coverslips at 1.3×10^4 cells/cm^2 while Clone 9 cells were seeded onto coverslips in 6-well dishes at $0.25–0.5 \times 10^6$ cells/well. Clone 9 cells were cultured for 1–3 days and WIF-B cells for 8–12 days until they reached maximal density and polarity (32).

Preparation of antibodies to MAL2

Rabbit polyclonal antibodies were made against a peptide corresponding to amino acids 13–23 of rat MAL2 and affinity purified by Covance Research Products (Denver, PA). To verify specificity of the antibody, peptide competition experiments were performed. In a final volume of 100 μl of PBS containing 1% BSA, 1 μg affinity purified antibody was incubated with a 10-fold molar excess of peptide. The mixture was incubated on ice for 2–4 h stirring occasionally by inverting and was used directly for immunofluorescence labeling or further diluted (1:4000) in PBS/BSA for immunoblotting.

Virus production and infection

Recombinant adenoviruses for pIgA-R, DPPIV and HA were generated using the Cre-Lox system as described (31). Recombinant MAL2 adenoviruses and MAL2 anti-sense viruses were generated using the ViraPower Adenoviral Expression System according to the manufacturer's instructions (Invitrogen). For the anti-sense construct, the first two-thirds of MAL2 was PCR-amplified with primers that have additional sequences that encode the recombination sites in the reverse order from how they appear in the Invitrogen Gateway® vector. Thus, when recombined, the fragment inserted in the opposite, anti-sense orientation, which was verified by plasmid sequencing. WIF-B or Clone 9 cells were infected with recombinant adenovirus for 60 min at 37°C as described (31). The cells were washed with complete medium and incubated an additional 16 – 20 h to allow expression.

Immunoblotting

In general, samples were mixed with Laemmli sample buffer (33) and boiled for 3 min. Because boiling abolished MAL2 immunoreactivity (data not shown), samples to be immunoblotted for MAL2 were incubated in Laemmli sample buffer for 20 min at RT before loading. Proteins were electrophoretically separated using SDS-PAGE and

transferred to nitrocellulose and immunoblotted with the indicated antibodies. HRP-conjugated secondary antibodies were used at 5 ng/ml, and immunoreactivity was detected with enhanced chemiluminescence. Relative protein levels were determined by densitometric analysis of immunoreactive bands.

Immunoprecipitations

WIF-B cells grown on coverslips were lysed in 0.5 ml lysis buffer (300 mM NaCl, 25 mM $NaPO_4$, 20 mM octylglucoside and 0.5% TX-100, pH 7.4) containing 1 μg/ml each of antipain, leupeptin, benzamidine and PMSF and incubated on ice for 30 min. Lysates were cleared by centrifugation at 120,000 × g for 30 min at 4°C. Samples were incubated with 1.0 μg affinity-purified MAL2 antibodies overnight at 4°C. Protein-A Sepharose (20 μl of a 50% (v/v) slurry) was added for 2 h and samples processed as described (2). Unbound and bound fractions were separated by SDS-PAGE and transferred to nitrocellulose and immunoblotted for the indicated proteins.

Immunofluorescence microscopy

In general, control or infected cells were fixed on ice with chilled PBS containing 4% paraformaldehyde (PFA) for 1 min and permeabilized with ice-cold methanol for 10 min. Cells were processed for indirect immunofluorescence as previously described (34). Alexa 488- or 568-conjugated secondary antibodies were used at 3–5 μg/ml. Cells were treated for 1 h with 33 μM nocodazole to depolymerize microtubules. To deplete cholesterol, cells were treated for 60 minutes with 5 mM mβCD in serum-free medium at 37°C. To arrest the biosynthetic pathway, cells were treated with 50 μg/ml cycloheximide at 37°C for the indicated times. Labeled cells were visualized at RT by epifluorescence on an Olympus BX60 Fluorescence Microscope (OPELCO, Dulles, VA) using an UPlanFl 100x/NA 1.3, phase 3, oil immersion objective. Images were taken using a HQ2 CoolSnap digital camera (Roper Scientific, Germany) and IP Labs software v4.04 (BD Biosciences, Rockville, MD). Adobe Photoshop (Adobe Systems Inc, Mountain View, CA) was used to further process images and to compile figures.

Antibody labeling of live cells

Clone 9 cells were continuously labeled for 1 h with antibodies specific for 5'NT, pIgA-R or DPPIV (all 1:100) or endolyn (1:25). After washing three times for 2 minutes each with prechilled medium, cells were fixed and stained with secondary antibodies as described above. WIF-B cells were labeled for 30 min at 4°C with anti-pIgA-R or –DPPIV antibodies. After washing three times for 2 minutes each with prechilled medium, cells were incubated at 37°C for 1 h. Cells were fixed and stained with secondary antibodies as described above.

Recycling assays in Clone 9 cells

Apical antigens were labeled and chased as described above. To strip antibodies from their surface antigens, cells were rinsed briefly with prewarmed PBS and incubated in isoglycine (200 mM glycine, 150 mM NaCl, pH 2.5) for 5 min at RT. The cells were rinsed with PBS, placed in prewarmed complete medium and incubated at 37°C for the desired times. The total population of antibody-antigen complexes was detected with secondary antibodies in cells fixed as described above whereas the cell surface population was detected in cells fixed with 4% PFA in PBS for 30 min at RT.

Surface biotinylation

Clone 9 cells grown on coverslips were treated in the absence or presence of 50 μg/ml cycloheximide for the indicated times. Cells were cooled on ice for 5 min then incubated twice for 15 min each with prechilled 1 mg/ml NHS-biotin in borate buffer (10 mM borate,

137 mM NaCl, 3.8 mM KCl, 0.9 mM $CaCl_2$, 0.52 mM $MgCl_2$ and 0.16 mM $MgSO_4$, pH 9.0). Cells were quenched with prechilled 50 mM NH_4Cl made fresh in PBS for 10 min. Cells were lysed and extracted as described above for immunoprecipitations. Cleared lysates were incubated with 50 µl of a 50% slurry of streptavidin agarose for 2 h at 4°C. Samples were further collected and washed as described (2). Unbound and bound fractions were separated by SDS-PAGE and transferred to nitrocellulose and immunoblotted for the indicated proteins. The percent surface associated pIgA-R or DPPIV was determined from densitometric analysis of immunoreactive species.

Supplementary Material

Refer to Web version on PubMed Central for supplementary material.

Acknowledgments

We thank Dr. Ann Hubbard for providing the many antibodies and viruses used in this study. We thank Sai Ramnarayanan for technical assistance in preparing the MAL2 wildtype and anti-sense viruses and for critically reviewing the manuscript. This work was supported by the National Institutes of Health grants GM070801 and DK082890 awarded to PLT.

References

1. Tuma PL, Hubbard AL. Transcytosis: crossing cellular barriers. Physiol Rev. 2003; 83(3):871–932. [PubMed: 12843411]
2. Bartles JR, Feracci HM, Stieger B, Hubbard AL. Biogenesis of the rat hepatocyte plasma membrane in vivo: comparison of the pathways taken by apical and basolateral proteins using subcellular fractionation. Journal of Cell Biology. 1987; 105:1241–1251. [PubMed: 3654750]
3. Bartles JR, Hubbard AL. Plasma membrane protein sorting in epithelial cells: do secretory pathways hold the key? Trends in Biochemical Science. 1988; 13:181–184.
4. Schell MJ, Maurice M, Stieger B, Hubbard AL. 5'nucleotidase is sorted to the apical domain of hepatocytes via an indirect route. J Cell Biol. 1992; 119(5):1173–1182. [PubMed: 1447295]
5. Nyasae LK, Hubbard AL, Tuma PL. Transcytotic efflux from early endosomes is dependent on cholesterol and glycosphingolipids in polarized hepatic cells. Mol Biol Cell. 2003; 14(7):2689–2705. [PubMed: 12857857]
6. De Marco MC, Martin-Belmonte F, Kremer L, Albar JP, Correas I, Vaerman JP, Marazuela M, Byrne JA, Alonso MA. MAL2, a novel raft protein of the MAL family, is an essential component of the machinery for transcytosis in hepatoma HepG2 cells. J Cell Biol. 2002; 159(1):37–44. [PubMed: 12370246]
7. de Marco MC, Puertollano R, Martinez-Menarguez JA, Alonso MA. Dynamics of MAL2 during glycosylphosphatidylinositol-anchored protein transcytotic transport to the apical surface of hepatoma HepG2 cells. Traffic. 2006; 7(1):61–73. [PubMed: 16445687]
8. Marazuela M, Acevedo A, Garcia-Lopez MA, Adrados M, de Marco MC, Alonso MA. Expression of MAL2, an integral protein component of the machinery for basolateral-to-apical transcytosis, in human epithelia. J Histochem Cytochem. 2004; 52(2):243–252. [PubMed: 14729876]
9. Marazuela M, Alonso MA. Expression of MAL and MAL2, two elements of the protein machinery for raft-mediated transport, in normal and neoplastic human tissue. Histol Histopathol. 2004; 19(3):925–933. [PubMed: 15168355]
10. Marazuela M, Martin-Belmonte F, Garcia-Lopez MA, Aranda JF, de Marco MC, Alonso MA. Expression and distribution of MAL2, an essential element of the machinery for basolateral-to-apical transcytosis, in human thyroid epithelial cells. Endocrinology. 2004; 145(2):1011–1016. [PubMed: 14576188]
11. Wilson SH, Bailey AM, Nourse CR, Mattei MG, Byrne JA. Identification of MAL2, a novel member of the mal proteolipid family, though interactions with TPD52-like proteins in the yeast two-hybrid system. Genomics. 2001; 76(1–3):81–88. [PubMed: 11549320]

12. van ISC, Hoekstra D. (Glyco)sphingolipids are sorted in sub-apical compartments in HepG2 cells: a role for non-Golgi-related intracellular sites in the polarized distribution of (glyco)sphingolipids. J Cell Biol. 1998; 142(3):683–696. [PubMed: 9700158]

13. Hemery I, Durand-Schneider AM, Feldmann G, Vaerman JP, Maurice M. The transcytotic pathway of an apical plasma membrane protein (B10) in hepatocytes is similar to that of IgA and occurs via a tubular pericentriolar compartment. J Cell Sci. 1996; 109(Pt 6):1215–1227. [PubMed: 8799812]

14. Ihrke G, Martin GV, Shanks MR, Schrader M, Schroer TA, Hubbard AL. Apical plasma membrane proteins and endolyn-78 travel through a subapical compartment in polarized WIF-B hepatocytes. J Cell Biol. 1998; 141(1):115–133. [PubMed: 9531552]

15. Hunziker W, Male P, Mellman I. Differential microtubule requirements for transcytosis in MDCK cells. Embo J. 1990; 9(11):3515–3525. [PubMed: 2170116]

16. Tuma PL, Nyasae LK, Hubbard AL. Nonpolarized cells selectively sort apical proteins from cell surface to a novel compartment, but lack apical retention mechanisms. Mol Biol Cell. 2002; 13(10):3400–3415. [PubMed: 12388745]

17. Tall RD, Alonso MA, Roth MG. Features of influenza HA required for apical sorting differ from those required for association with DRMs or MAL. Traffic. 2003; 4(12):838–849. [PubMed: 14617347]

18. Boutros R, Fanayan S, Shehata M, Byrne JA. The tumor protein D52 family: many pieces, many puzzles. Biochem Biophys Res Commun. 2004; 325(4):1115–1121. [PubMed: 15555543]

19. Groblewski GE, Wishart MJ, Yoshida M, Williams JA. Purification and identification of a 28-kDa calcium-regulated heat-stable protein. A novel secretagogue-regulated phosphoprotein in exocrine pancreas. J Biol Chem. 1996; 271(49):31502–31507. [PubMed: 8940165]

20. Groblewski GE, Yoshida M, Yao H, Williams JA, Ernst SA. Immunolocalization of CRHSP28 in exocrine digestive glands and gastrointestinal tissues of the rat. Am J Physiol. 1999; 276(1 Pt 1):G219–G226. [PubMed: 9886999]

21. Kaspar KM, Thomas DD, Taft WB, Takeshita E, Weng N, Groblewski GE. CaM kinase II regulation of CRHSP-28 phosphorylation in cultured mucosal T84 cells. Am J Physiol Gastrointest Liver Physiol. 2003; 285(6):G1300–G1309. [PubMed: 12893633]

22. Martin-Belmonte F, Arvan P, Alonso MA. MAL mediates apical transport of secretory proteins in polarized epithelial Madin-Darby canine kidney cells. J Biol Chem. 2001; 276(52):49337–49342. [PubMed: 11673461]

23. Martin-Belmonte F, Martinez-Menarguez JA, Aranda JF, Ballesta J, de Marco MC, Alonso MA. MAL regulates clathrin-mediated endocytosis at the apical surface of Madin-Darby canine kidney cells. J Cell Biol. 2003; 163(1):155–164. [PubMed: 14530381]

24. Martin-Belmonte F, Puertollano R, Millan J, Alonso MA. The MAL proteolipid is necessary for the overall apical delivery of membrane proteins in the polarized epithelial Madin-Darby canine kidney and fischer rat thyroid cell lines. Mol Biol Cell. 2000; 11(6):2033–2045. [PubMed: 10848627]

25. Aroeti B, Casanova J, Okamoto C, Cardone M, Pollack A, Tang K, Mostov K. Polymeric immunoglobulin receptor. Int Rev Cytol. 1992; 137B:157–168. [PubMed: 1478818]

26. Breitfeld PP, Casanova JE, McKinnon WC, Mostov KE. Deletions in the cytoplasmic domain of the polymeric immunoglobulin receptor differentially affect endocytotic rate and postendocytotic traffic. J Biol Chem. 1990; 265(23):13750–13757. [PubMed: 2380185]

27. Casanova JE, Apodaca G, Mostov KE. An autonomous signal for basolateral sorting in the cytoplasmic domain of the polymeric immunoglobulin receptor. Cell. 1991; 66(1):65–75. [PubMed: 2070419]

28. Casanova JE, Breitfeld PP, Ross SA, Mostov KE. Phosphorylation of the polymeric immunoglobulin receptor required for its efficient transcytosis. Science. 1990; 248(4956):742–745. [PubMed: 2110383]

29. Mostov KE. Transepithelial transport of immunoglobulins. Annu Rev Immunol. 1994; 12:63–84. [PubMed: 8011293]

30. Ramnarayanan SP, Cheng CA, Bastaki M, Tuma PL. Exogenous MAL Reroutes Selected Hepatic Apical Proteins into the Direct Pathway in WIF-B Cells. Mol Biol Cell. 2007

31. Bastaki M, Braiterman LT, Johns DC, Chen YH, Hubbard AL. Absence of direct delivery for single transmembrane apical proteins or their "Secretory" forms in polarized hepatic cells. Mol Biol Cell. 2002; 13(1):225–237. [PubMed: 11809835]

32. Shanks MS, Cassio D, Lecoq O, Hubbard AH. An improved rat hepatoma hybrid cell line. Generation and comparison with its hepatoma relatives and hepatocytes in vivo. J Cell Sci. 1994; 107:813–825. [PubMed: 8056838]

33. Laemmli UK. Cleavage of structural proteins during the assembly of the head of bacteriophage T4. Nature. 1970; 227(5259):680–685. [PubMed: 5432063]

34. Ihrke G, Neufeld EB, Meads T, Shanks MR, Cassio D, Laurent M, Schroer TA, Pagano RE, Hubbard AL. WIF-B cells: an in vitro model for studies of hepatocyte polarity. J Cell Biol. 1993; 123(6 Pt 2):1761–1775. [PubMed: 7506266]

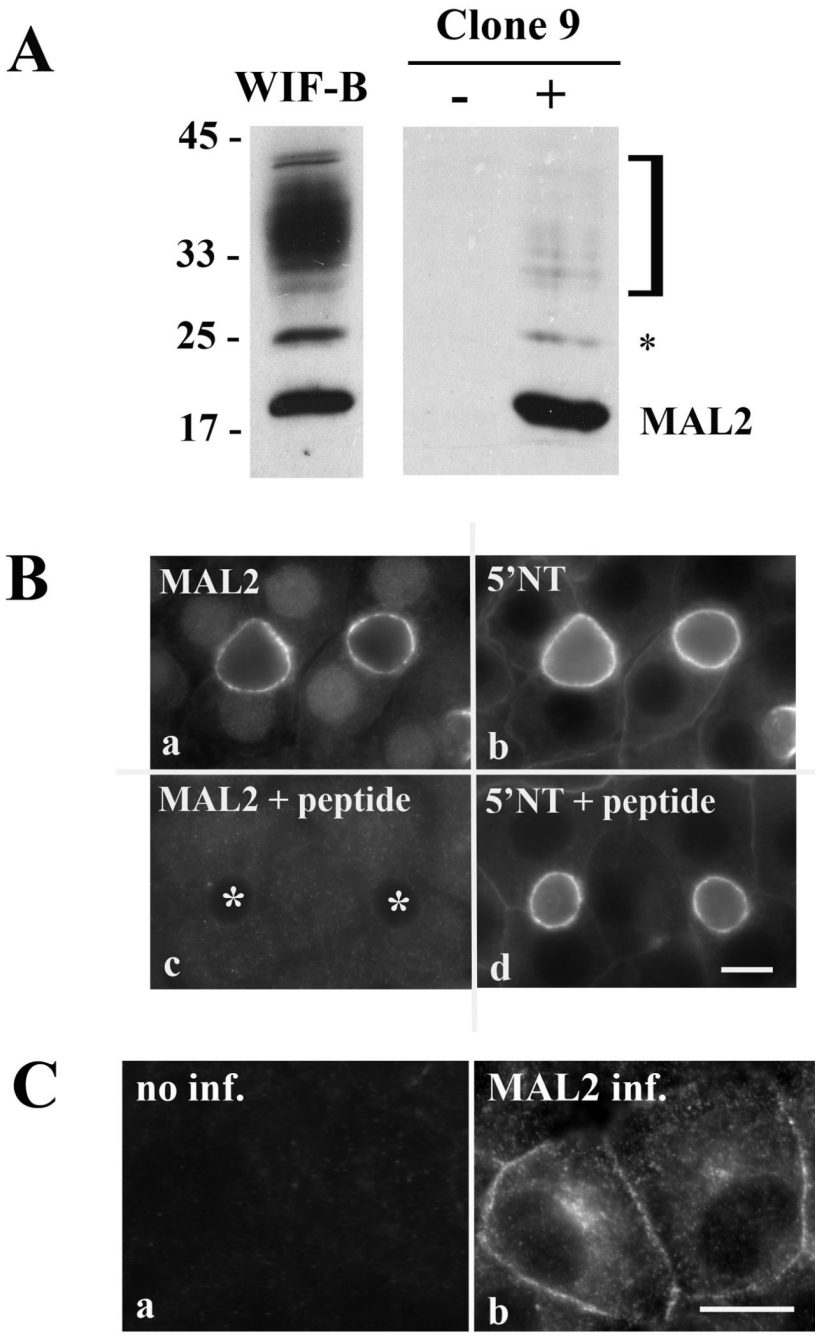

Figure 1. The peptide antibody specifically detects MAL2

(A) WIF-B or Clone 9 (control or exogenously expressing MAL2) cell lysates were immunoblotted for MAL2. The bracket highlights a 30–38 kDa diffuse set of bands that has been described by others and the asterisk indicates a 25 kDa species also detected by others (see text). (B) WIF-B cells were immunolabeled with MAL2 antibodies that were preabsorbed in the absence (a) or presence (c) of a 10-fold molar excess of peptide against which the MAL2 antibodies were generated. Cells were double labeled for 5'NT (b and d). Preabsorption specifically abolished MAL2 apical labeling. Asterisks are marking selected BCs. (C) Clone 9 cells were infected with recombinant adenovirus expressing MAL2 (b).

Control and infected cells were labeled with MAL2 antibodies. Only infected cells were stained further confirming the specificity of our antibodies. Bar, 10 μM.

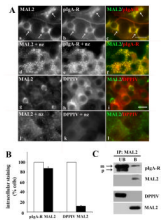

Figure 2. MAL2 co-distributes with exogenously expressed pIgA-R, but not DPPIV

(A) Cells were infected with recombinant adenovirus expressing pIgA-R (a–f) or DPPIV (g–l). After 20 h of expression, cells were immunolabeled for MAL2 (a, d, g) and pIgA-R (b and e) or DPPIV (h and k). In d –f and j–l, cells were treated for 60 min with 33 μM nocodazole (nz) and images were focused at the cell periphery. Merged images are shown (c, f , i and l). Bar, 10 μM. (B) pIgA-R or DPPIV overexpressing WIF-B cells were scored for the presence of intracellular puncta positive for the indicated protein. Values are expressed as the mean ± SEM. Measurements were performed on at least three independent experiments. (C) WIF-B lysates from cells overexpressing pIgA-R or DPPIV were co-immunoprecipitated with 1 μg affinity-purified MAL2 antibodies. Unbound (UB) and bound (B) fractions were immunoblotted for MAL2 or pIgA-R and DPPIV as indicated. Arrows are pointing to the mature (m) and precursor (p) forms of pIgA-R

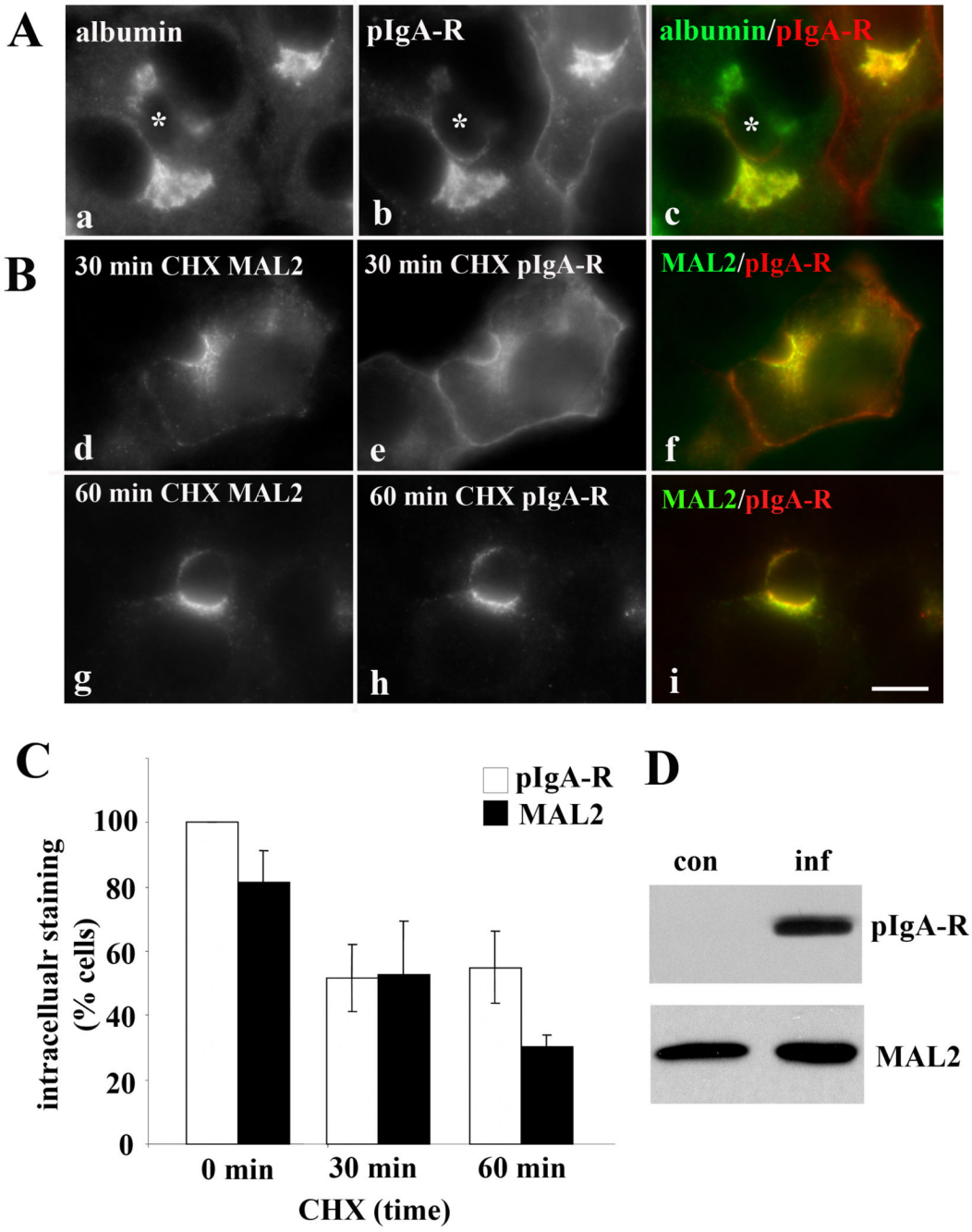

Figure 3. MAL2 and overexpressed pIgA-R are present in the biosynthetic pathway

(A) WIF-B cells were infected with recombinant adenovirus expressing pIgA-R for 20 h. Cells were labeled for albumin (a) and pIgA-R (b). The merged image shows overlapping staining at the Golgi (c). (B) WIF-B cells exogenously expressing pIgA-R were incubated for the indicated times with 50 μg/ml cycloheximide (CHX). Cells were fixed and stained for MAL2 (d and g) and pIgA-R (e and h). Merged images are shown (f and i). Asterisks are marking selected BCs. Bar, 10 μM. (C) WIF-B cells overexpressing pIgA-R were treated with 50 μg/ml CHX for the indicated times and scored for the presence of intracellular puncta positive for pIgA-R or MAL2. Values are expressed as the mean ± SEM. Measurements were performed on at least three independent experiments. (D) WIF-B

(control or exogenously expressing pIgA-R) cell lysates were immunoblotted for pIgA-R (top panel) or MAL2 (bottom panel). No changes in MAL2 levels were observed.

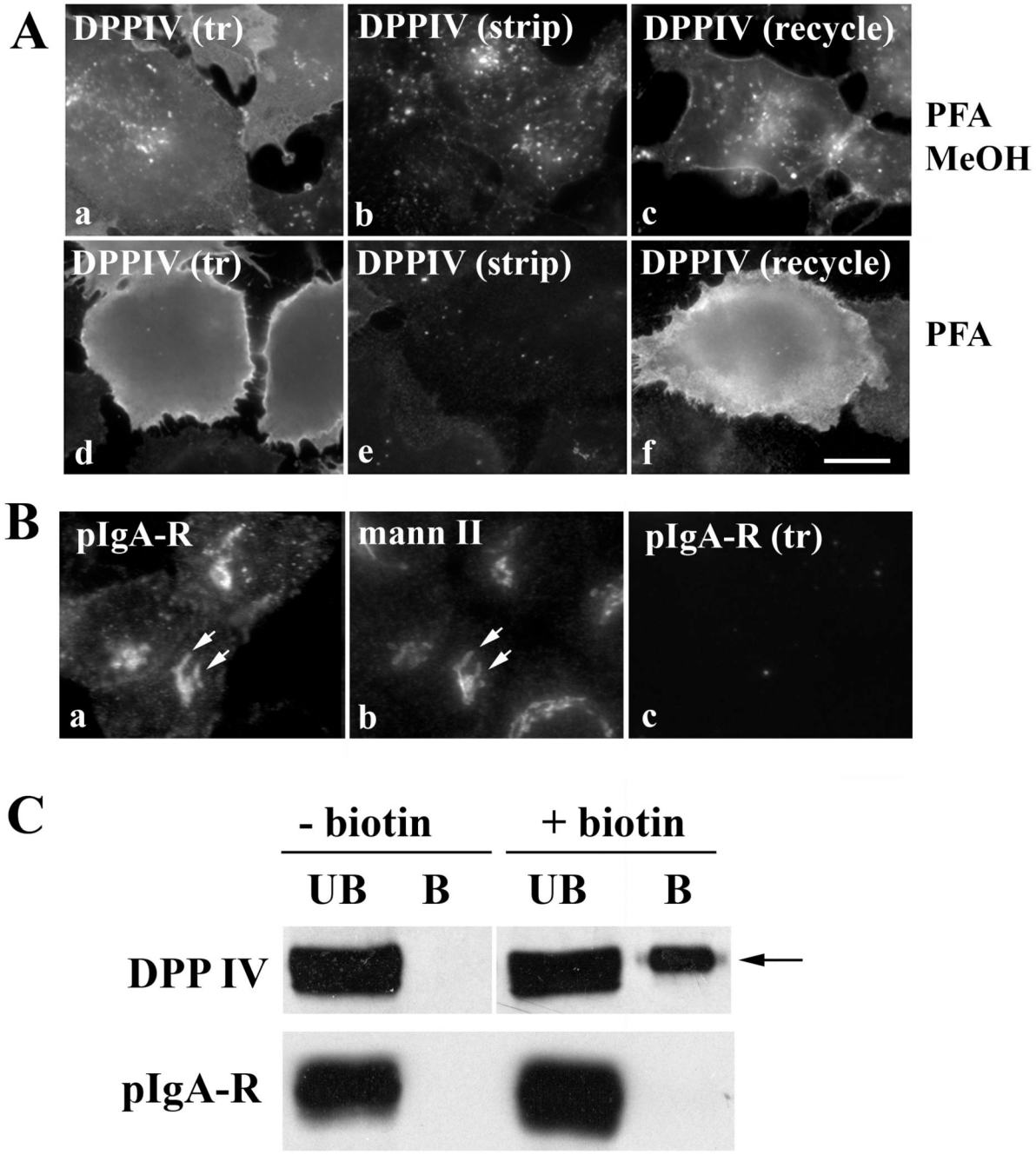

Figure 4. In the absence of MAL2, DPPIV, but not pIgA-R, reaches the plasma membrane in Clone 9 cells

(A) Clone 9 cells expressing exogenous DPPIV were surface-labeled with anti-DPPIV antibodies, and the antibody-antigen complexes trafficked (tr) for 1 h at 37°C (a and d). The remaining membrane-associated antibodies were stripped with isoglycine for 5 min at RT (b and e). Only the internalized DPPIV-antibody complexes were detected (b). Cells were incubated an additional hour at 37°C (c and f) to allow recycling. To detect the entire population of trafficked antibodies, cells were fixed and permeabilized (PFA/MeOH) (a–c). To detect only the antigens present at the cell surface, cells were fixed in 4% PFA for 30 min at RT (d–f). Bar, 10 μm (B) Clone 9 cells exogenously expressing pIgA-R were double

labeled for steady state (ss) distributions of pIgA-R (a) and mannosidase II (mann II) (b). Arrows are pointing to Golgi structures containing pIgA-R. In c, cells were continuously labeled with anti-pIgA-R antibodies for 60 min for 37°C. Cells were fixed and permeabilized and labeled to detect the trafficked (tr) antibody. No pIgA-R was detected. Bar, 10 μm (C) Clone 9 cells overexpressing DPPIV and pIgA-R were treated in the absence or presence of 1 mg/ml biotin as indicated (see Materials and Methods). Cells were lysed and incubated with streptavidin-agarose. The unbound (UB) and bound (B) samples were immunoblotted for DPPIV and pIgA-R as indicated. The arrow is marking the mature form of DPPIV.

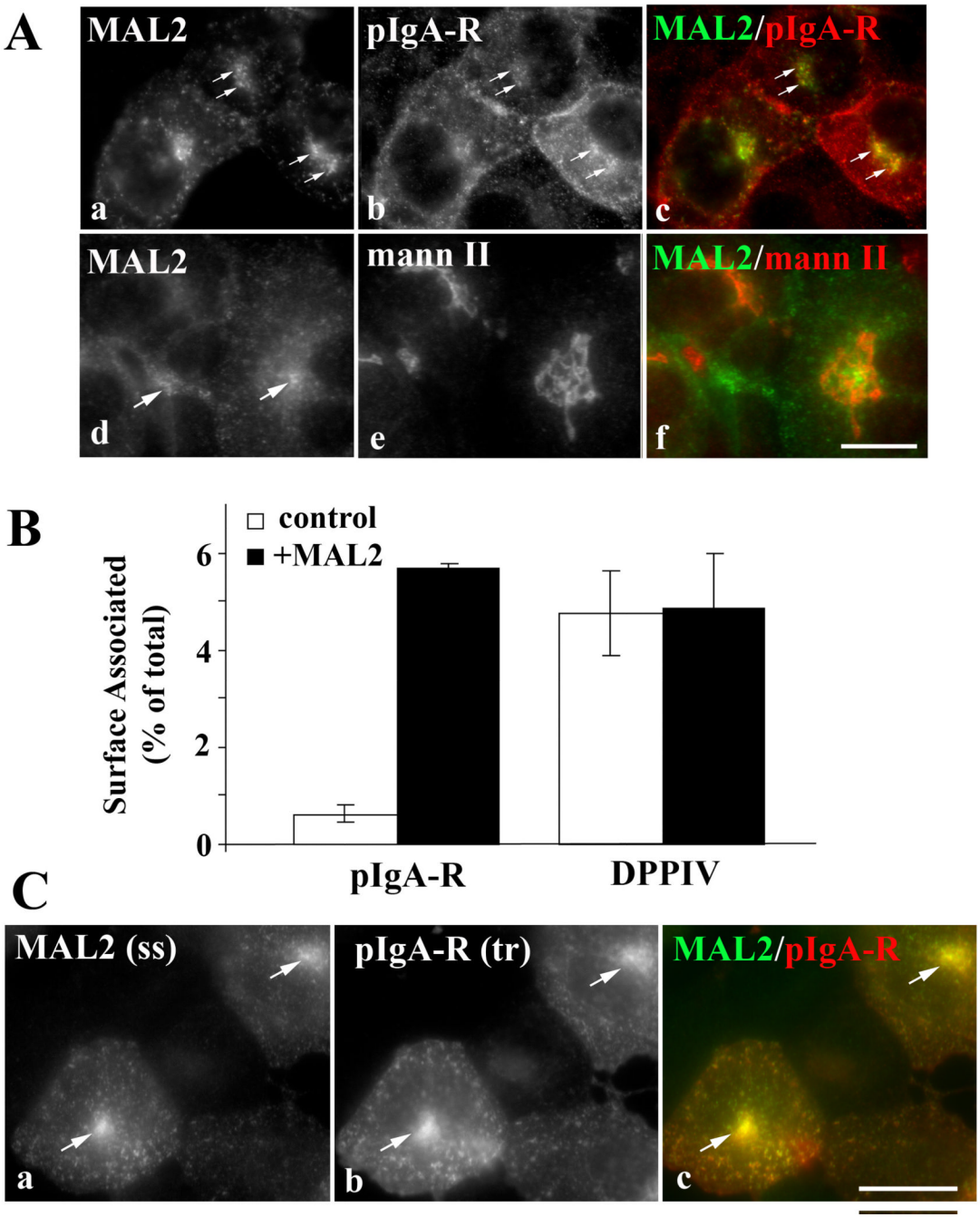

Figure 5. MAL2 expression in Clone 9 cells redistributes pIgA-R to the plasma membrane

(A) Clone 9 cells were infected with both pIgA-R and MAL2 recombinant adenoviruses (a–f). After 20 h of expression, cells were stained for the steady state (ss) distributions of MAL2 and pIgA-R (a–c) or MAL2 and mannosidase II (mann II) (d–f). Arrows are pointing to puncta that contain both MAL2 and pIgA-R (a–c) or only contain MAL2 (d–f). (B) Clone 9 cells were infected with DPPIV or pIgA-R recombinant adenovirus alone (open bars) or with MAL2 (black bars). After 20 h of expression, cells were surface biotinylated (see Materials and Methods). Cells were lysed and incubated with streptavidin-agarose. The unbound and bound samples were immunoblotted for pIgA-R or DPPIV and the percent surface association was determined by densitometric analysis of immunoreactive bands.

Values are expressed as the mean ± SEM. Measurements were done on at least three independent experiments. (C) Cells were continuously labeled with anti-pIgA-R antibodies for 60 min for 37°C. Cells were fixed and permeabilized and labeled to detect steady state (ss) MAL2 distributions and the trafficked (tr) pIgA-R. Bar, 10 μm

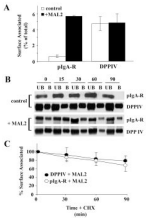

Figure 6. MAL2 expression is required for pIgA-R delivery from the Golgi to the plasma membrane in Clone 9 cells

(A) Clone 9 cells were infected with DPPIV or pIgA-R recombinant adenovirus alone or with MAL2 as indicated. After 20 h of expression, cells were treated with 50 μg/ml cycloheximide for the indicated times. Cells were chilled on ice and surface biotinylated (see Materials and Methods). Cells were lysed and incubated with streptavidin-agarose. The unbound (UB) and bound (B) samples were immunoblotted for pIgA-R or DPPIV as indicated. Representative immunoblots are shown from at least three independent experiments. (B) The percent surface association of DPPIV and MAL2 was calculated from densitometric analysis of immunoreactive bands as shown in A. The 0 min values were set to 100% and the percent of pIgA-R or DPP IV that remained surface associated was calculated. Values are expressed as the mean ± SEM. Measurements were done on at least three independent experiments.

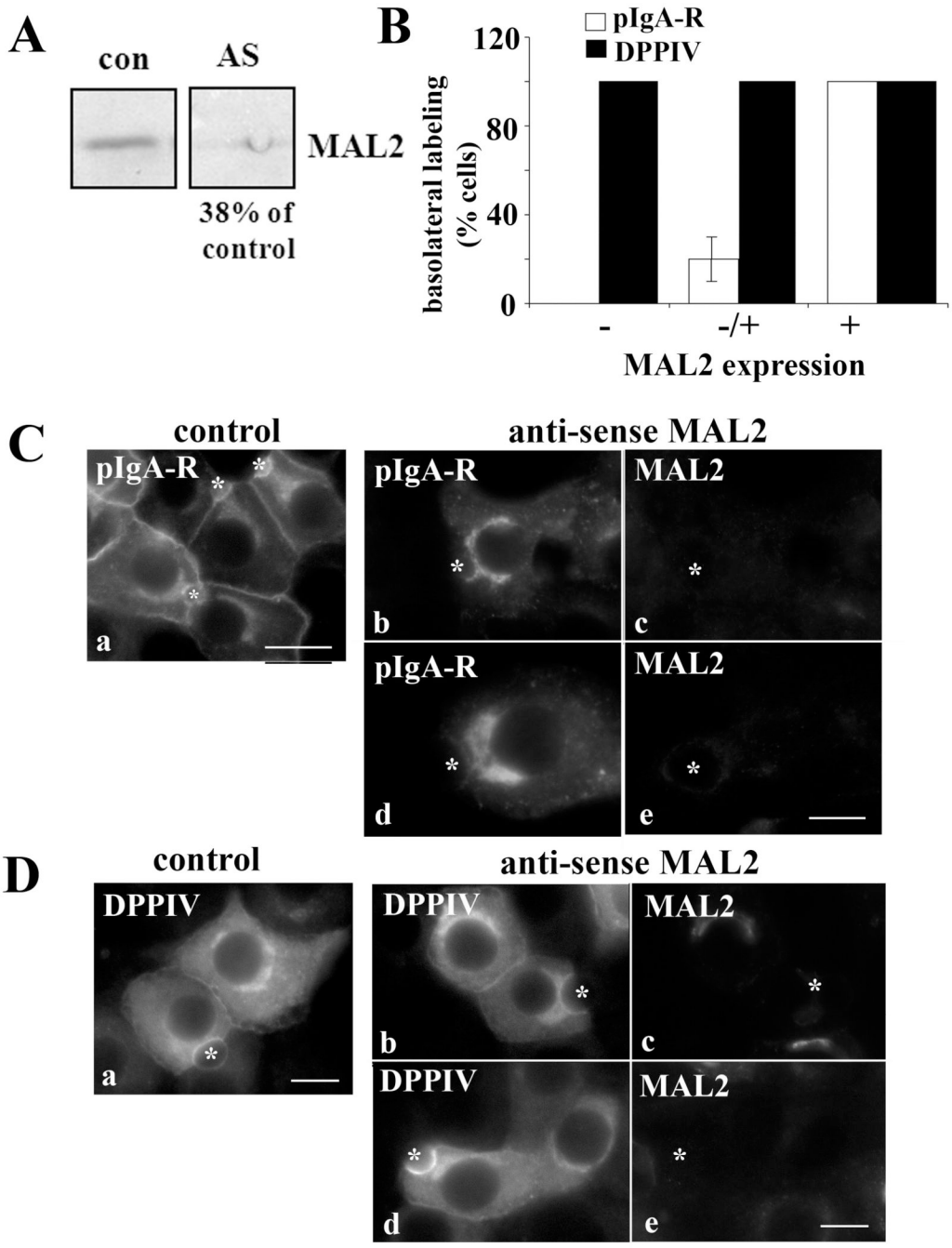

Figure 7. In WIF-B cells with MAL2 expression knocked down, pIgA-R, but not DPPIV, is present only in the Golgi

(A) Lysates from control (con) or MAL2 antisense virus (AS) expressing cells were immunoblotted for MAL2. WIF-B cells were infected with pIgA-R (C) or DPPIV (D) alone or with MAL2 anti-sense adenoviruses (B–D) for 60 min as indicated. After 20 h, cells were fixed and labeled for pIgA-R, DPPIV or MAL2 as indicated. Asterisks are marking selected BCs. Bar, 10 μm. In B, The percent cells positive for pIgA-R or DPPIV basolateral labeling was determined for cells expressing no (−), low (−/+) and normal (+) levels of MAL2. The calculations for pIgA-R were performed on three independent experiments. Values are

expressed as the mean ± SEM. The calculations for DPPIV were performed on two independent experiments. Values represent the average.

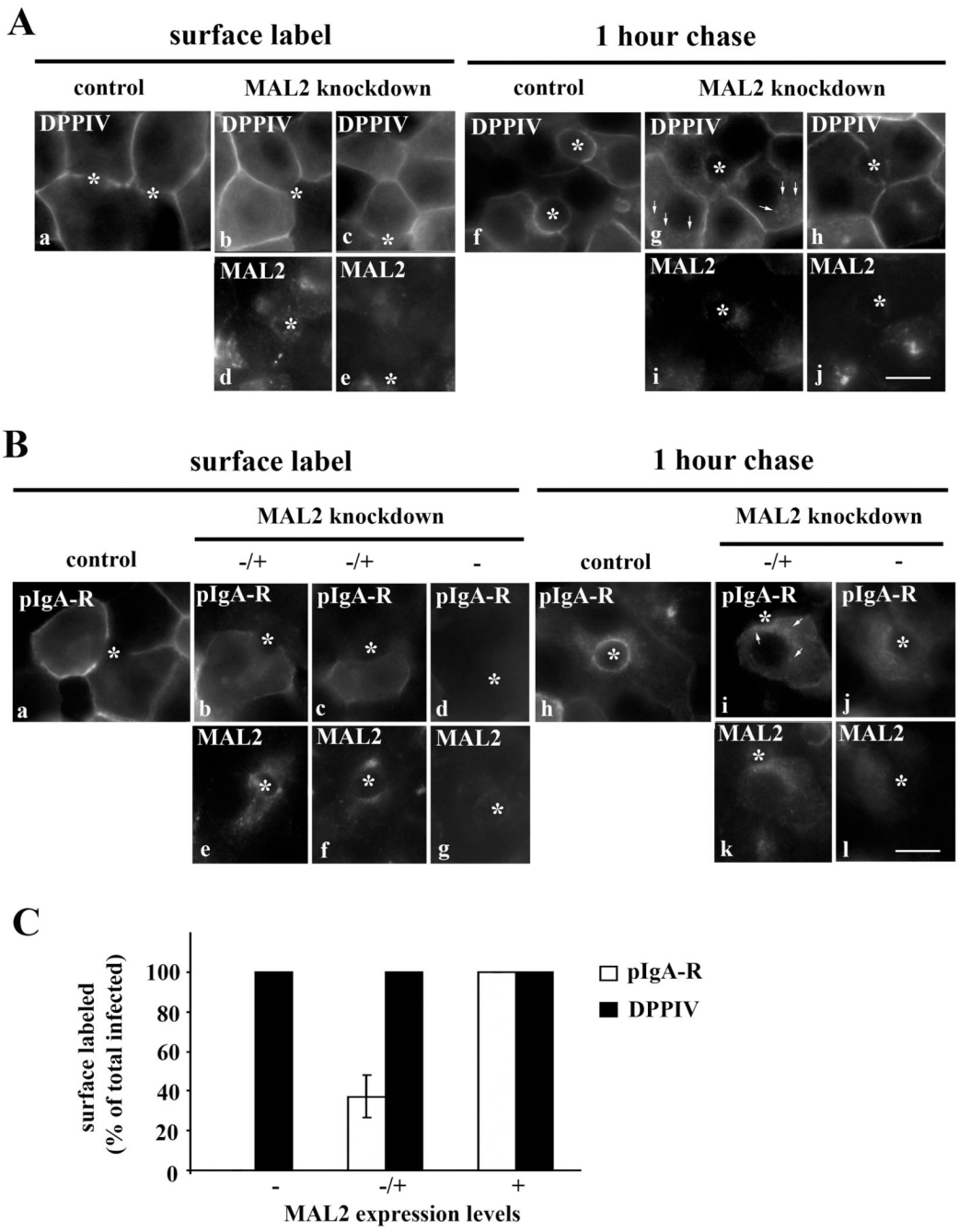

Figure 8. MAL2 knockdown in WIF-B cells inhibits basolateral delivery of pIgA-R, but not DPPIV, yet DPPIV transcytosis is impaired

WIF-B cells were infected with DPPIV (A) or pIgA-R (B) alone or with MAL2 anti-sense adenoviruses for 60 min as indicated. After 20 h, DPPIV or pIgA-R were surface-labeled for 30 min at 4°C (A, a–c; B, a–d) with specific antibodies. Antibody-antigen complexes were chased for 1 h at 37°C (A, f–h; B, h–j). Cells were fixed and permeabilized and labeled to detect the trafficked antibody. Arrows are marking intracellular puncta in MAL2 knockdown cells. Asterisks are marking selected BCs. Bar, 10 μM In C, the percent cells positive for pIgA-R or DPPIV basolateral labeling was determined for cells expressing no

(−), low (−/+) and normal (+) levels of MAL2. The calculations were performed on at least three independent experiments. Values are expressed as the mean ± SEM.